PERFORMANCE OF BATTERY CHARGE CONTROLLERS AN INTERIM TEST REPORT

Ward I. Bower
Sandia National Laboratories
Albuquerque, NM 87185

James P. Dunlop
Craig W. Maytrott
Florida Solar Energy Center
Cape Canaveral, FL 32920

SAND--90-1300C

DE90 011413

ABSTRACT

The performance of battery charge controllers and their effects on the system are a critical concern for stand-alone photovoltaic systems with battery storage. Many types of charge controllers are being marketed today, and designers need to understand more about their performance and compatibility with different kinds of batteries and systems.

This paper describes the evaluations and selected interim test results from eight different models of small (approx. 10 amps) charge controllers. They are being subjected to a comprehensive test program including thorough electrical characterizations at selected temperatures, photovoltaic inputs and load levels. After electrical characterizations, the charge controllers are divided into concurrent evaluation paths. One path consists of side-by-side operational systems tests in which the charge controllers are installed in identical stand-alone PV systems. The other path consists of continuous environmental and electrical cycling in which the controllers are subjected to programmed electrical inputs, temperatures, and relative humidities. Recharacterizations of all controllers are performed on a periodic basis to detect changes in electrical performance. In addition, selected custom tests are performed on identical models to determine response to transients, installation issues and system compatibilities. The data presented here include measured electrical characteristics of the controllers, temperature effects, operational performance, and interface measurements at the array, battery and load.

INTRODUCTION

Sandia National Laboratories and the Florida Solar Energy Center are currently undertaking an extensive program to evaluate charge controllers for stand-alone photovoltaic (PV) systems. The objective of the program is to test commercially available charge controllers under a variety of simulated and actual operating conditions experienced in PV systems. The goals of the program are to impact positively the development of charge controllers through feedback to the manufacturers and to develop criteria for design and application that will ultimately improve PV system reliability and battery subsystem performance.

The charge controllers selected for the test program are nominal 12—volt, 10—amp units with a typical cost of less than $200. The controllers include a variety of solid-state and mechanical switching types, shunt and series regulators, most with

---

low voltage load disconnect and some with external temperature compensation (1). Table 1 gives a list of the charge controllers selected for the initial testing program and their general characteristics.

Table 1. Charge Controllers Under Test

Manufacturer	Model	Amps Volts	Regulator Type	Low Voltage Disconnect	Temp. Comp.
Bobier Electronics	M-8	8 A 12 V	Series Relay	Yes LVD-8	None
Balance of Systems Specialists	SS12 10DRE	10 A 12 V	Shunt Solid-State	Yes	Ext.
Heliotrope General	CC-10	10 A 12 V	PWM Series Solid-State	No	Int.
Integrated Power	TT1 12DH	10 A 12 V	Shunt Solid-State	No	Ext.
Polar Products	SSC-200 12-06	6 A 12 V	Series Solid-State	Yes	Ext.
Sandia Labs	SL-1	10 A 12 V	Series Solid-State	Yes	Ext.
Specialty Concepts	ASC 12/7E	7 A 12 V	Shunt Solid-State	Yes	Int.
Sun Amp Power	PBR12 12LC-10	12 A 12 V	Shunt Solid-State	Yes	Int.

Stand-alone PV systems employing storage batteries may fall into one of several operational categories. Examples range from simple lighting systems with high average insolation and comparatively small loads to systems such as remote weekend cabins, where both insolation and loading are unpredictable. In general, systems with predictable, small, continuous loads can be designed to operate without a battery charge controller or a low-voltage disconnect (2). Proper design can limit charging currents to safe and effective equalizing values (C/50 flooded or C/100 sealed) without the need for a charge controller. Any system, however, that has unpredictable loads, user intervention, optimized or undersized (for cost) battery storage, or any characteristics that would allow excessive battery overcharging or over-discharging needs a charge controller and/or a low-voltage load disconnect (LVD) (3).

Selection criteria for a charge controller should include consideration of the following items:

- o Low voltage disconnect (LVD)
- o High voltage array disconnect (HVD) or limiting
- o Battery chemistry, characteristics, size and costs
- o Thermal environment
- o PV array type, characteristics and size
- o Wire sizes and lengths
- o Load criticality
- o Life cycle and O&M costs

The combination of control algorithms and setpoints (thresholds) for managing the current flow into a battery, the temperature or current compensation of those algorithms or setpoints, and the hysteresis between setpoints determine the effectiveness of a charge controller in a PV/battery power system. The setpoint and algorithm for disconnecting the load when a battery becomes discharged can also have a great influence on the life of a battery and the availability of the load. When a charge controller is used in a PV/battery power system, it should provide a maximum of charge transfer from the PV array to the battery while minimizing deep cycling of the battery and protecting the battery from overcharge. The addition of a charge controller should improve the life-cycle cost of the system.

The life of a lead-acid battery is proportional to the average state-of-charge of the battery so long as the battery is not overcharged or overdischarged. Other factors that affect the life of a lead-acid battery are temperatures, cell construction, the depth of discharge before recharge, and contamination of the cell chemistry (3,4,5). A typical flooded, deep-cycle, lead-acid battery that is maintained above 90% state-of-charge (SOC) can provide two to three times more charge/discharge cycles than a battery allowed to reach 50% SOC before recharging. Similar and more dramatic results are found with sealed and lead-calcium alloyed grid batteries. A system using a gelled or starved electrolyte storage battery is more likely to require a charge controller. Plate constructions greater than 0.25 inch thick have been shown to minimize the effects of sulfation (2,3). The gelled or starved electrolyte cell design is less tolerant to overcharging, since there is limited excess electrolyte for electrolysis and the gasses produced can create sufficient pressure to rupture seals allowing permanent electrolyte loss (5). Table 2 summarizes characteristics of typical batteries used in stand-alone PV systems.

Table 2. Battery Characteristics

Type	Life	Cycling	Gassing	Initial Cost
Lead-Antimony	Fair	Good	Medium	Low
Lead-Calcium	Fair	Poor	Low	Low

Lead-Selenium	Good	Excellent	Medium	Low
Nickel-Cadmium	Excellent	Excellent	High	High

A charge controller should allow installer (not user) adjustments of setpoints or algorithms to accommodate different types of batteries or it should be clearly labeled and sold for a specific type of battery. The unpredictability and uncertainty of available energy from a PV system require optimizing charge transfer from the PV to the battery, and good overcharge protection for the battery. When an unpredictable load is coupled to a PV/battery power source, a charge controller must also prevent overdischarging of the battery.

A charge controller must be very reliable because a failure generally shortens the life of a battery. Often the cost of transportation to remote sites to replace a battery is an order of magnitude higher than the cost of the battery. The life cycle costs of a system often are doubled by the need to replace batteries, especially in remote locations. The charge controller must also be functionally reliable and must provide a rugged, corrosion-resistant interface connection to the remainder of the system.

The basic circuit topologies for charge controllers include series or shunt regulators (6). The regulating elements may be controlled by simple voltage setpoints, pulse-width-modulation (PWM) or integration algorithms. The cost of the charge controller is dependent on the sophistication of control, but must be a factor in the system design. Figure 1 shows the shunt-type controller and Fig. 2 shows the series-type controller. Both show locations for an optional LVD.

Fig. 1. Shunt regulator with load disconnect.

Fig. 2. Series regulator with load disconnect.

A required component in the shunt regulator is a blocking diode between the battery and regulator switch to prevent shorting the battery when the switch closes. The switch may be a solid-state semiconductor or an electromechanical relay. The duty cycle of the average current flow through the switch alters the effective operating point on the PV array I-V curve with a resulting controlled flow of charge into the battery. The algorithms for controlling the switch may be voltage setpoint driven, PWM as a function of battery voltage, or any variation of voltage, current or temperature compensated control methods. The load disconnect may not be included in the charge controller package and is not needed for some applications. The load disconnect may appear in the positive or negative battery-to-load connections. Most shunt regulators use negative leg switching when solid-state switching is used.

Grounding is typically on the negative side of the battery since many loads use the case as a negative ground. The National Electrical Code should be followed and caution used with the controllers using negative leg switching (8). Multiple grounds may disable the LVD functions in some cases.

The series regulator may use solid-state or electromechanical switches. A blocking diode may not be necessary in a series regulator. Many low-voltage systems (depending on components chosen) will not experience high reverse current losses at night. Losses incurred by using a blocking diode may be higher than reverse current losses. All higher voltage systems (> 24 V) need blocking diodes unless the switch, with the proper control algorithm, prevents current flow to the array at night. Algorithms for controlling the regulating switch are as varied as those for shunt regulator topologies. The load disconnects also may or may not be included in the controller, and techniques for controlling the load disconnect are similar to designs for shunt controllers.

OBJECTIVES

The objectives of this evaluation are listed below. The charge controllers were purchased by specifying the battery type and system configuration to the suppliers. The controllers were evaluated at the Florida Solar Energy Center and Sandia National Laboratories. Objectives were to:

1. Provide design-related information, conclusions, and operational experience (i.e., failure rates and mechanisms) for PV/battery charge controllers.

2. Provide manufacturers with information on possible hardware improvements.

3. Determine the safety of the hardware under normal/extreme operating modes and list possible failure modes and resultant system impacts.

4. Show hardware limitations and compatibilities via performance evaluations at environmental extremes under controlled conditions.

5. Determine the general construction quality of the hardware.

DESCRIPTION OF THE EVALUATIONS

The evaluation program consists of four phases; characterization tests, systems tests, environmental and electrical cycling tests and custom tests. The custom tests are conducted at Sandia National Laboratories; all other tests are conducted at the Florida Solar Energy Center.

Electrical Characterization Tests

The characterization testing is designed to determine the setpoints or switching thresholds at which control functions are initiated by the charge controllers at various temperatures and load conditions. These setpoints include the PV array high voltage disconnect (HVD), the PV array reconnect voltage (RCV), the low-voltage load disconnect (LVD), and the load reconnect voltage (LRV). The tests involve inputing simulated PV array operating conditions and then ramping the battery voltage from 10 to 16 volts, then back to 10 volts while the controller is connected to a load and the simulated PV array. These characterizations are performed, at 5, 25 and 45 °C with temperature compensation probes first inside and then outside the environmental chamber, when applicable. In addition, the coulombic and energy efficiencies for the controllers are determined as a function of the battery voltage.

A computer-controlled facility was developed, complete with custom software and hardware, that electrically simulates a PV array, battery, and load, as well as controls an environmental chamber. The simulated PV array is an integrated-software I-V curve program-controlled interface to a programmable unipolar regulated voltage and current power supply. The simulated 12-volt battery is a 24-volt battery-bank-driven, high-power op-amp circuit capable of sourcing or sinking sufficient current to maintain a software programmed battery voltage ramping waveform. The load is a menu-driven, computer-controlled, Darlington-switched parallel power resistor load bank. The power supply and load bank are forced-air cooled, while the op-amp for the battery simulator is water cooled. The environmental chamber has separate proportional-integral-derivative control loops for heating and cooling the air and water tray for temperature and humidity control. The environmental chamber controller is RS-232 interfaced to the computer's integrated-software temperature control setpoints.

The array is programmable up to 20 volts open-circuit, 10 amps short-circuit, with a programmed fill factor of 0.65. The battery voltage starts at a programmable minimum and is slowly increased to a programmable maximum, then slowly returned to the minimum. Current into or out of the battery allows the battery voltage to follow the ramp. The load may be stepped in 2 1/2 amp steps from 0 to 10 amps. The environmental chamber is allowed to stabilize at a given temperature for one hour before any data are taken. This allows a massive charge controller to thermally stabilize prior to test. The chamber temperature is held at 5, 25, or 45 °C for test points. Figure 3 shows a block diagram of the characterization test set-up.

Fig. 3. Test setup for charge controller characterizations.

On a quarterly basis, all controllers will be taken out of the systems tests and environmental/electrical cycling tests for recharacterization. This schedule will be followed through the duration of the test program to examine drift in controller setpoints and failure modes.

Environmental and Electrical Cycling Tests

After the characterization testing, one from each of the eight pairs of controllers is subjected to temperature, humidity and electrical cycling to identify potential failures. The environmental and electrical cycling tests are described in Fig. 4.

Fig. 4. Environmental and electrical cycling tests.

Systems Tests

Concurrent with the electrical and environmental cycling tests, one from each of the eight pairs of controllers was installed in actual PV systems to examine operational characteristics, real-time performance, effects on the battery subsystem and availability of the load.

Each of the eight systems was configured identically with the exception of the charge controller. The battery used in the systems is a flooded deep-cycle, lead-calcium/lead-antimony hybrid design, nominally rated at 12 V, 100 Ah at a C/20 discharge rate. PV modules, measured at the controller, were a nominal 50 watts at 15.7 volts and 3.15 amps maximum power at 25 °C. They were used to charge the batteries and operate the charge controllers at about 33% of their rated current. A resistive load, set at 18 ohms to produce a nominal 0.65 amp load current was selected to balance the expected energy availability of the system based on local insolation data. Fig. 5 shows a block diagram of the systems test configuration.

Fig. 5. Systems test configuration for charge controllers.

In order to examine the effects of the different charge controllers on the batteries, all eight batteries were purchased at the same time and have consecutive serial numbers, indicating consistency in manufacturing and shelf life prior to the tests. To verify consistency, the batteries were initially float charged in series using a constant voltage, current-limiting power supply to bring all batteries up to 100% SOC. In addition, the batteries were individually weighed to quantify water loss, and the specific gravity readings were recorded. The batteries were then subjected to a discharge capacity test by cycling a resistive load at a nominal C/25 rate (4 amps) to 10.7 volts per battery, on for two hours then off for one hour to allow the voltages to stabilize. Integration of the amp-hours discharged from the batteries showed a lower limit of 99 amp-hours and an upper limit of 108 amp-hours, or about an 8-9% difference, indicating performance consistency among the batteries. After the capacity tests, the batteries were again fully recharged to begin operation of the system tests.

Custom Tests

The custom tests were designed to subject the controllers to atypical conditions that may be experienced in stand-alone PV systems. These tests include voltage and current transients, susceptibility to and generation of electromagnetic interference (EMI), the ability to operate a variety of inductive and other non-resistive loads, and self-protection features of the controllers.

The custom tests measured parameters such as switching characteristics, load compatibility, surge effects, connection sequences, loss of battery, temperature compensation, adjustment ranges, grounding criteria and mechanical and environmental construction of the hardware. Custom tests are continuing to measure EMI susceptibility and radiation, voltage transient protection effectiveness, parallel operation effects and compatibility, and other parameters that need attention in the course of these evaluations.

RESULTS OF CHARGE CONTROLLER EVALUATIONS

Results of Cycling Tests

All 16 controllers were characterized at all allowable specified temperature and electrical combinations. One controller had an initial operational problem that was resolved by replacement of its temperature probe. A terminal connection fell off one unit because of an insufficient number of exposed threads. Four units (2 models) did not go into array disconnect at some conditions. ~~A variety of~~ accuracy varied ~~was seen for~~ array disconnect temperature compensation. One hundred-twelve hysteresis graphs were produced from 492 unique tests. A hysteresis graph shows battery current as a function of battery voltage with a current scale of +/- 12 amps and a voltage scale of 10 to 15 volts. Figure 6 shows a family of hysteresis curves for a shunt-type controller with LVD at 5, 25 and 45 °C for a 5 amp PV and load current.

Fig. 6. Hysteresis plot for shunt-type controller.

Electrical and environmental cycling tests were conducted for a two-month period concurrent with the systems tests. The tests proved uneventful, with no electrical or mechanical failures documented.

Results of Systems Tests

During the first few weeks of the systems tests, the PV modules were not delivering their rated output current to the battery and load. Further investigation of the module I-V characteristics determined that modules were operating at a higher

voltage than the maximum power voltage, or to the right of the 'knee' on the I-V curve. This situation presents a potential problem area for low-voltage stand-alone PV systems. The problem typically arises from the combination of low maximum power voltage modules exacerbated by voltage drop in the system wiring, fuses, disconnects, blocking diodes and charge controller. In this case, if the system is sized based on the current at maximum power, the result will be under-utilization of the PV array, and the battery will seldom see a complete recharge and will operate at a lower average SOC. This promotes sulfation and a reduction in battery life.

In application, this operating condition has self-regulating characteristics, due to the reduction in module current as the battery and array operating voltage increases beyond the maximum power voltage. This technique is often used in small low-voltage and low-power systems in which the use of a charge controller is not desirable, due to reliability or cost concerns. However, this type of design requires careful determination of the wide range of temperatures, system currents and the effects of system voltage drops on the array operating point. The use of a charge controller with low-voltage modules can further reduce module operating voltage due to voltage drop, and special attention must be paid to the operating voltage on the module I-V curve.

Although this reduction in PV current would have detrimental effects over the long term for most systems that are marginally sized, this was not a problem during the system tests because of above-normal insolation. All charge controllers experienced a high-voltage disconnect several times during this period, and the batteries were never discharged below 80% SOC.

After a few weeks of operation and data collection with the lower voltage PV modules, the original modules were changed for new modules with a higher maximum power voltage to attain more effective module current utilization. Figure 7 shows the effects of voltage drop on the operating point for the original and replacement PV modules.

Fig. 7. Operating characteristics of the PV modules.

After a week of operation with the new modules, all eight of the PV modules were disconnected to allow the load to discharge the batteries and allow the charge controllers to activate the LVD if so equipped. The range of load disconnect voltages varied between 11.49 and 12.18 volts, indicating a different level of load availability and battery treatment for the different systems. Once all the LVDs had been achieved, the loads were manually disconnected from the systems and the PV modules were allowed to charge the batteries over several days.

Once all charge controllers had regulated the PV array current for several days at the high-voltage point, the batteries were assumed to have all been fully charged. However, specific gravity readings at this time indicated that some batteries had low SOC even though the HVDs had been activated for all systems for several days. The maximum battery voltages achieved for the systems varied between 14.15 and 15.24 volts for the eight controllers under test.

To examine the existing SOC at this time, another capacity test was conducted. This indicated a significant difference in the available capacity of the batteries, ranging from 65 to 100 amp-hours, or roughly 65 to 100% of the original measured

capacity. To substantiate these results, the batteries were then fully recharged with the constant voltage, current limited power supply and subjected to yet another capacity test to determine if there were any problems with the batteries. Results of this capacity test compared well with the initial capacity tests, ranging from 99 to 105 amp-hour. Table 3 shows the battery characteristics at the conclusion of the systems tests.

Table 3. Battery Characteristics After Systems Tests.

System #	HVD	Max Voltage	Spec. Grav.	SOC %
1	14.3	14.31	1.25	86.7
2	14.2	14.15	1.18	64.4
3	14.5	14.60	1.26	92.4
4	14.2	14.40	1.21	71.0
5	13.7	14.22	1.19	70.6
6	14.6	14.66	1.26	95.6
7	14.1	14.19	1.18	65.8
8	--	15.24	1.28	99.8

The data were reviewed to find potential causes for the 35% SOC difference between the batteries at the conclusion of the systems tests. The most significant cause is suspected to be the high-voltage array disconnect setpoints for the respective charge controllers. There was a direct correlation between the maximum battery voltage achieved during the systems tests and battery SOC at the conclusion of the tests. The lowest remaining battery SOC occurred for the system with the lowest battery maximum voltage, and the highest battery SOC occurred in the system with the highest battery maximum voltage. This correlation did not apply to charge controllers with current-limiting high-voltage disconnects.

Although the charge controllers were purchased by specifying the type of batteries to be used, in some cases the high-voltage array disconnect, or maximum battery voltage achieved was too low to allow the batteries to fully recharge. However, some consideration must be given to the relative values of the array current and battery capacity and potential effects on battery charging and overcharging. In this case, some type of current compensated voltage setpoints may be desirable for the optimal control algorithm. Control algorithms will be investigated in future tests.

Results, Custom Test Evaluations

All of the shunt controllers tested used solid-state switches to close the circuit that shorts the PV array. All heat sinks were sized for in-spec thermal operating conditions of the semiconductor devices. The greatest heat dissipation in the shunt controller occurred when the battery was nearly fully charged and the PV source was

active. Voltage and current waveforms were monitored to determine the switching times and the characteristics of shunting the array and then removing the shunt from the array. The tests were conducted with an actual PV array. Most controllers shunted and unshunted the array in smooth fashion with switching times varying from 10 usec to 300 msec. One controller was found to have interactions lasting 10 usec between the input and output terminals during switching but this did not affect the operation of the power system.

Load compatibility with charge controllers is normally only a problem when load current passes through a disconnect switch. The combination of high surge starting currents and a low SOC battery was found to create a relaxation oscillation condition with several of the controllers. Figure 8 shows an inverter load on a charge controller exhibiting a small hysteresis (< 1 volt) between the LVD and LRV setpoints.

Fig. 8. Shunt controller oscillations with inverter load at low battery SOC.

The load switch may be solid-state or electromechanical but must be capable of interrupting dc currents at the rated voltage with inductive loads, such as motors or relays. The switch must also be able to withstand motor starting and power supply surges when power is reconnected to the system. Loads tested included a 1/6 hp dc motor, a 1/20 hp dc motor, an inverter connected to various loads up to the rating of the controller, fluorescent lights with dc ballasts, and resistive loads. All of the controllers with low-voltage battery cutoff switches were found to be compatible with the selected loads and able to handle starting surges and inductive kicks. Minor switch bounce was observed with hardware using the electromechanical switch. Controllers using a solid-state switch turned loads on and off in a smooth manner. Either type was found to be acceptable for system compatibility.

The series-type controllers selected for these evaluations exhibited a wide variety of switch types and algorithms. A linear control with a solid-state semiconductor was used on two of the units. One has voltage setpoints to control the battery voltage at a predetermined float level while the other unit sensed battery voltage and then switched to a constant current float condition at a preselected value modified by temperature and battery current and voltage. Other algorithms included a variable PWM scheme that was dependent upon battery voltage measured at the charge controller.

The series regulators used heatsinks, except for one in which the switching element was a relay. The heat sinks were properly sized, and heating was evident only when the unit was regulating. One unit included an overtemperature sensor that temporarily shut the system down in the case of overheating (70 °C). Overheating would only occur with full array inputs and very large loads for long periods of time.

Voltage and current waveforms of the array, battery and load were monitored under most operating conditions. Switching characteristics were recorded and appeared normal in all cases. One unit using a solid-state disconnect switch was found to oscillate when the battery SOC became low enough to initiate the LVD. Figure 9 shows a sample of the oscillation with a dc motor load. No damage to the load or the controller resulted during the test, but prolonged operation would cause heating in

both the load and controller. All hardware tested was compatible with the motor loads, dc fluorescent lamp ballasts, inverter loads and resistive loads.

Fig.9. Series controller oscillation with low battery SOC and motor load.

The setpoints and hysteresis of the charge controllers were measured in the custom tests in addition to the characterization tests. The custom tests allowed a more comprehensive evaluation of the setpoints with different battery sizes and with various loads. The adjustability and temperature coefficients of the probes and of the internal circuitry in each unit were also monitored. Only two of the units had user-adjustable setpoints. The setpoint adjustment using dip switches was the easiest to use and could easily be adjusted in field applications. The other unit using potentiometers was difficult to adjust with setpoint interactions being observed. Field changes or setups would be extremely difficult with this unit.

The measurement of the setpoints and algorithms of the controllers revealed a wide range of operating limits at ambient temperature and with temperature fluctuations. The range of measured factory set thresholds and the range of temperature coefficients are listed in Table 4. The range of preset factory adjustments for the HVD are consistent with the recommended 2.35 to 2.4 volts per cell at 25 °C, but the adjustable units with 13.18 to 15.28 volt ranges would allow misadjustment in the field with shortened battery lifetime. The charge controllers evaluated include a mix of units, some of which provided internal or external (battery) temperature compensation for the setpoints and also others that provided no temperature compensation.

Table 4. Charge Controller Setpoint Measurements

Setpoint	Temp (°C)	Range of Measured Setpoints	Range of Measured Temp Coefficients
LVD	25	11.48 to 11.89 V	-0.001 to 0.004 V/°C/cell
LRV	25	12.43 to 13.57 V	-0.004 to 0.005 V/°C/cell
HVD	25	13.90 to 14.54 V	-0.0044 to 0.0 V/°C/cell
RCV	25	12.61 to 13.45 V	^ V = 1.5 to 1.8 V

CONCLUSIONS AND FUTURE EVALUATION PLAN

All charge controllers demonstrated fair consistency between measured and manufacturer's setpoint data. Although some adjustable charge controller setpoints were as much as 0.5 volt off manufacturer specifications, all factory preset units were within 0.3 volt of specifications. This indicated that no faulty units were evaluated. One controller required initial field adjustment.

This paper presents interim results for a comprehensive test program for PV system battery charge controllers. After two months of testing, only limited conclusions can be addressed. The most significant conclusion is that some controllers did not maintain the battery SOC at a high level, even when loads were disconnected.

Further testing will evaluate the potential for overcharging the batteries by those controllers that maintained the batteries at a high SOC during the initial tests. An important finding of these evaluations is that only one failure was discovered during the initial characterizations. No significant drift of the thresholds or setpoints has been observed. No significant corrosion has been found. System interactions and design criteria will be reviewed to estimate system performance and cost impacts, and the data and results will be discussed with manufacturers. Many aspects of the evaluations have been touched here, and there is still much to be learned with further evaluations.

ACKNOWLEDGMENTS

The authors thank all who have contributed to this project, particularly Paul D. Freen for his work in developing the PV array simulator and battery simulator used for these evaluations and for his characterization test software development. Thanks also to Don Kilfoyle for his contributions on the side-by-side systems tests and to Stephen J. Harrington of Ktech Corp. for many customized tests needed to complete these evaluations.

REFERENCES

1. Strong, Steven J., The Solar Electric House, A Design Manual for Home-Scale Photovoltaic Power Systems, Rodale Press, 1987.

2. Allen, W.R. et al., "Evaluation of Solar Photovoltaic Energy Storage for Aids to Navigation," CG-D-5-81, United States Coast Guard, NTIS, Springfield, VA, 1981.

3. Vinal, George W., Storage Batteries, Fourth Edition, John Wiley & Sons, New York, NY., 1965.

4. Exide Management and Technology Company, Handbook of Secondary Storage Batteries and Charge Regulators in Photovoltaic Systems - Final Report, for Sandia National Laboratories, SAND81-7135, August 1981.

5. Trenchard, S.E., "Lead-acid Batteries in Solar Photovoltaic Power Systems for Marine Aids to Navigation," CG-DF-04-82, United States Coast Guard, NTIS, Springfield, VA, 1982.

6. Bechtel National, Inc., Handbook for Battery Energy Storage in Photovoltaic Power Systems, Final Report, SAND80-7022, February 1980.

7. Naval Facilities Engineering Command, Maintenance and Operation of Photovoltaic Power Systems, NAVFAC MO-405.1, September 1989.

8. National Fire Protection Association, National Electrical Code, 1990 Edition.

TYPES OF CHARGE CONTROLLERS FOR PV SYSTEMS

SHUNT REGULATOR

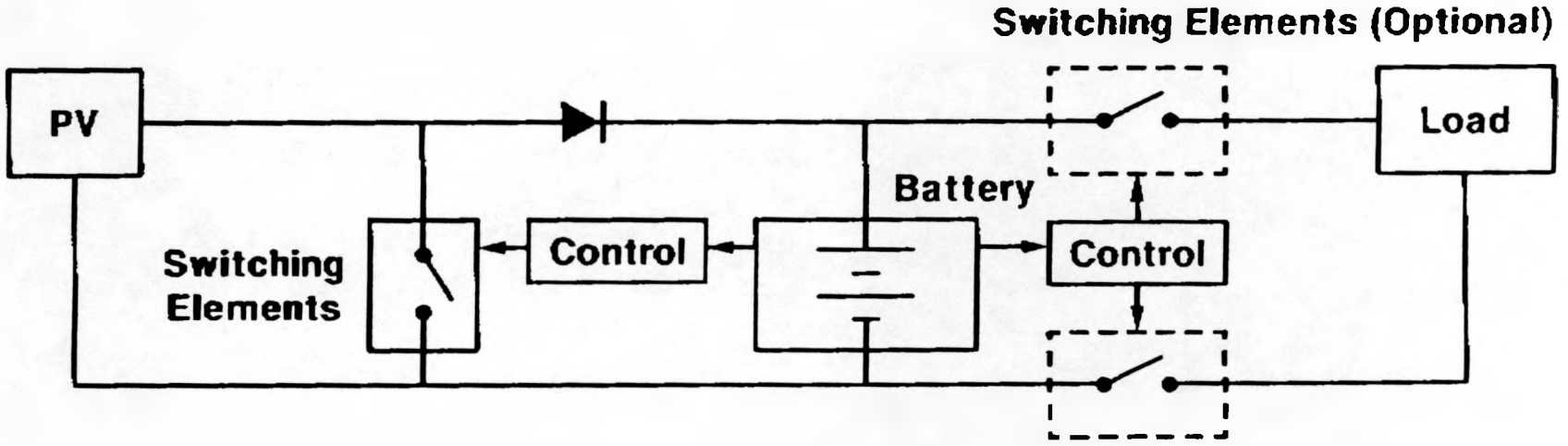

Switching Elements - Relays
Transistors
MOS FETs

Switching Techniques - PWM
Controlled for Thresholds
Linear

89S6000.02

TYPES OF CHARGE CONTROLLERS FOR PV SYSTEMS

SERIES REGULATOR

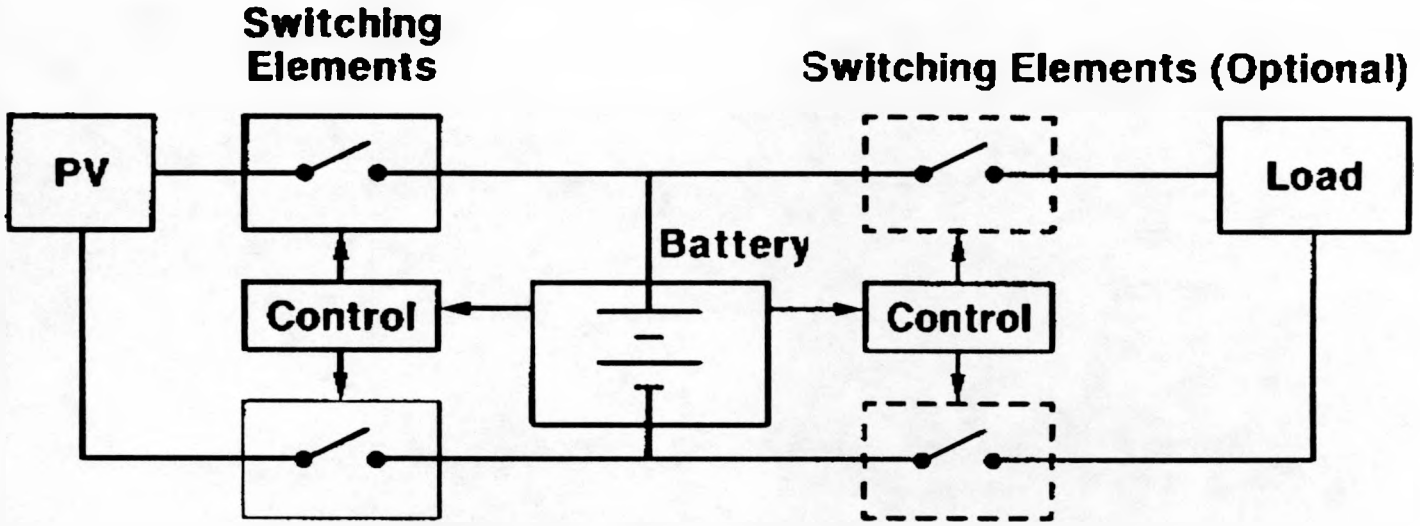

Switching Elements - Relays
Transistors
MOS FETs

Switching Techniques - PWM
Controlled for Thresholds
Linear
Slope

89S6000.03

Fig 2

CHARGE CONTROLLER CHARACTERIZATIONS

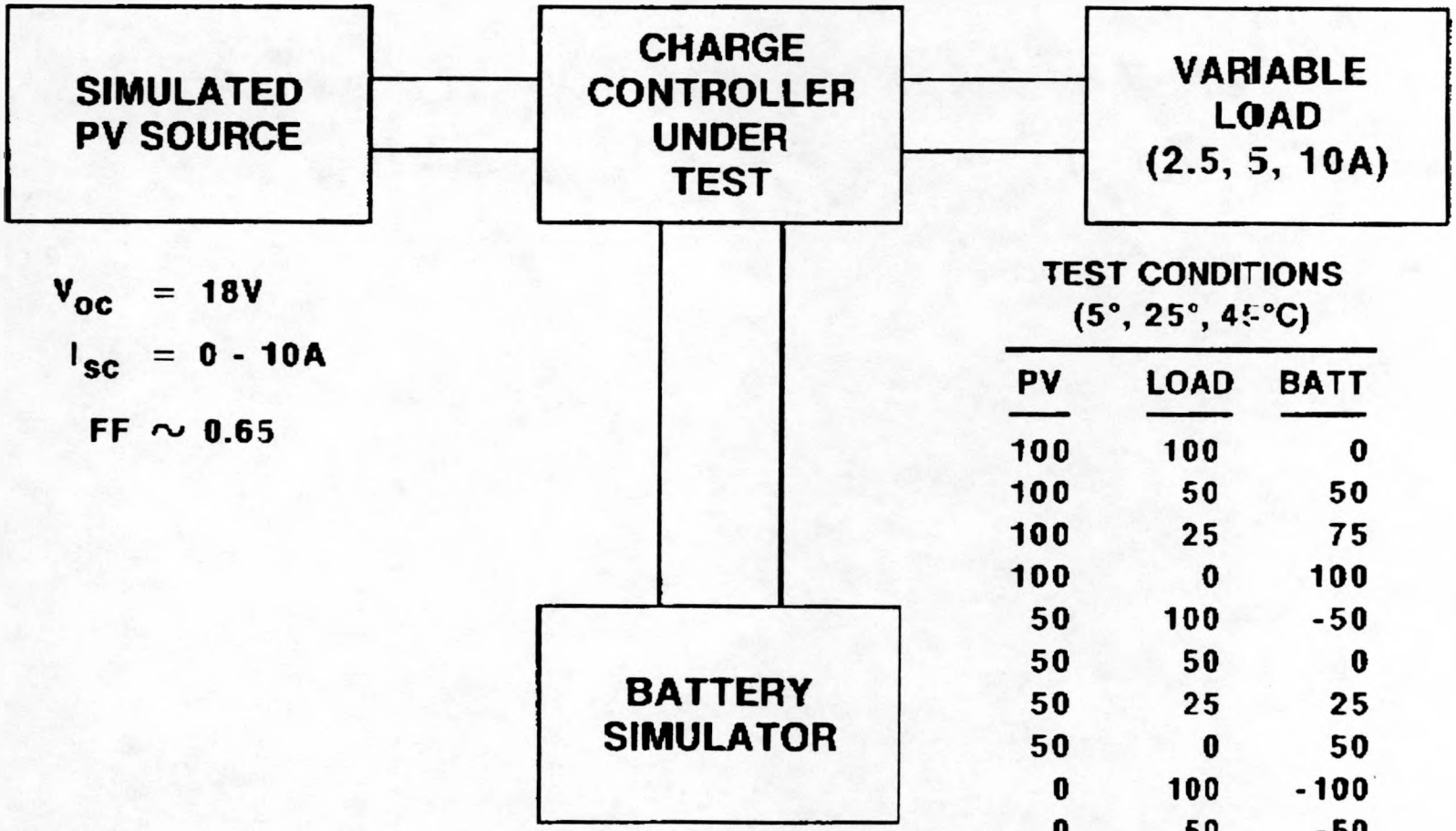

TEST CONDITIONS
(5°, 25°, 45°C)

PV	LOAD	BATT
100	100	0
100	50	50
100	25	75
100	0	100
50	100	-50
50	50	0
50	25	25
50	0	50
0	100	-100
0	50	-50
0	25	-25
0	0	0

90D6000.05

CHARGE CONTROLLER ACCELERATED TESTS

ELECTRICAL CYCLE

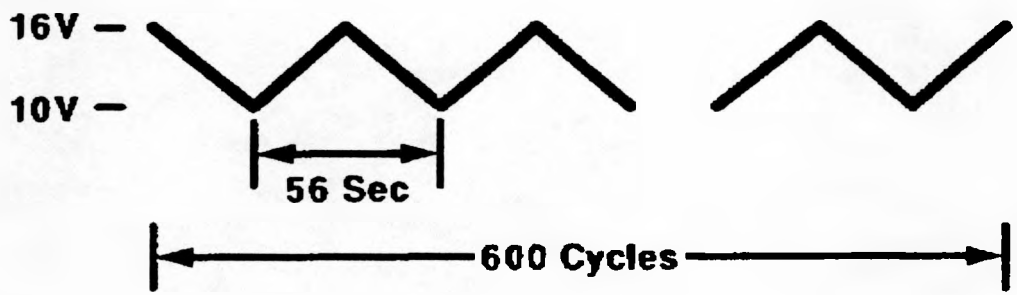

46,285 Cycles/mo.

2A Array Current

4A Load Current

TEMPERATURE PROFILE

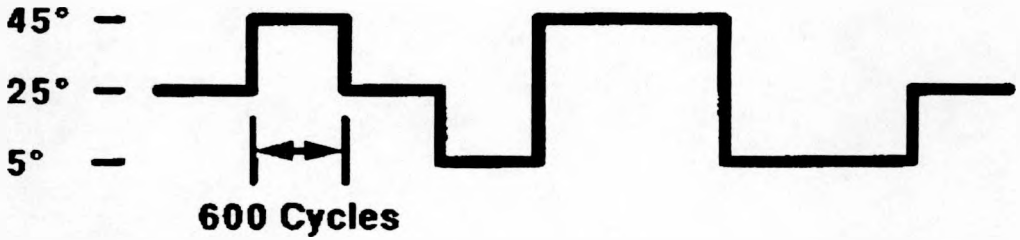

8.5 Cycles/mo.

238 hrs at each temperature

RELATIVE HUMIDITY PROFILE

8.5 Cycles/mo.

238 hrs at 50% R.H.

476 hrs at 95% R.H.

9006000.07

CHARGE CONTROLLER SYSTEM EVALUATIONS

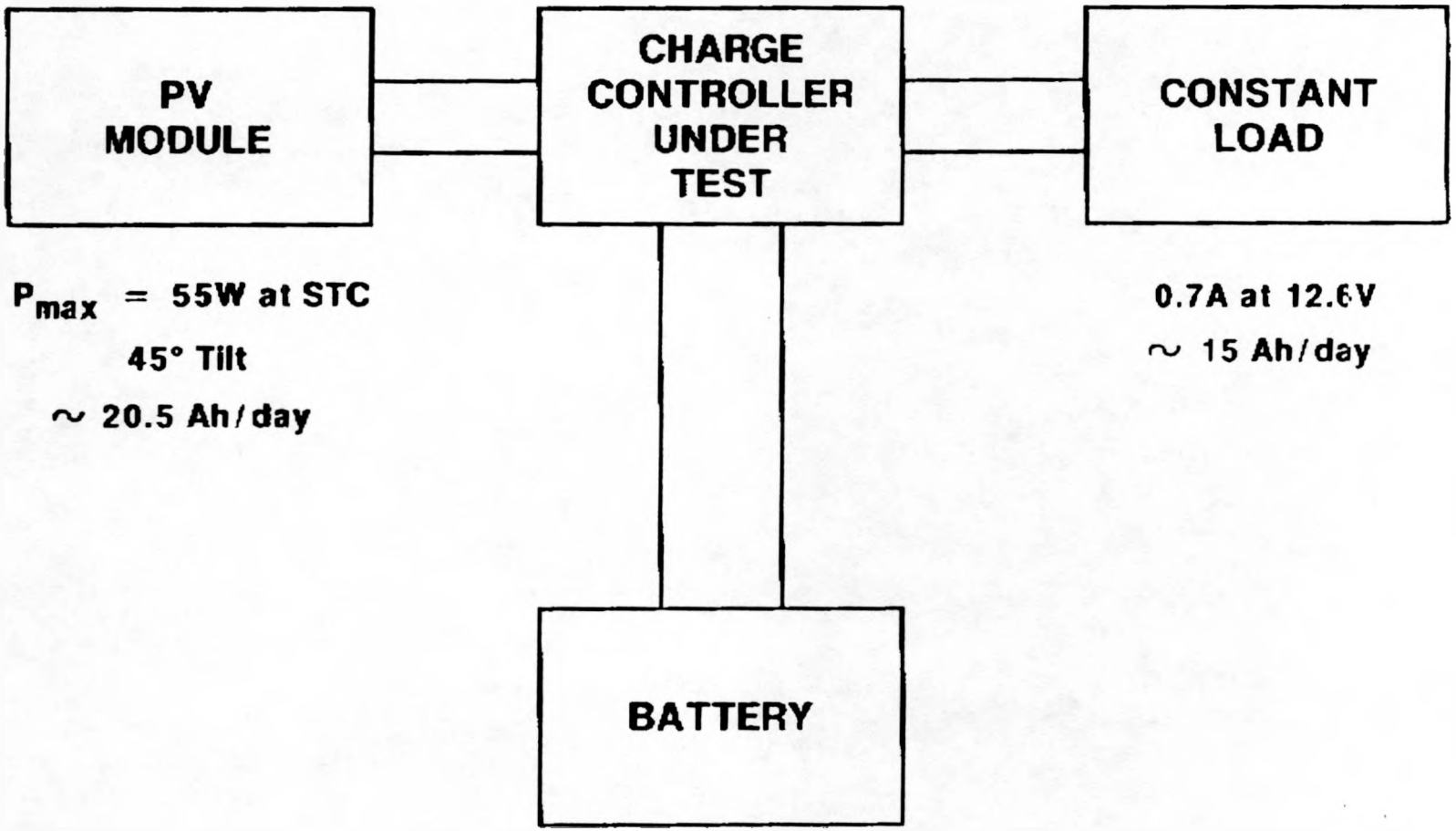

90D6800.05

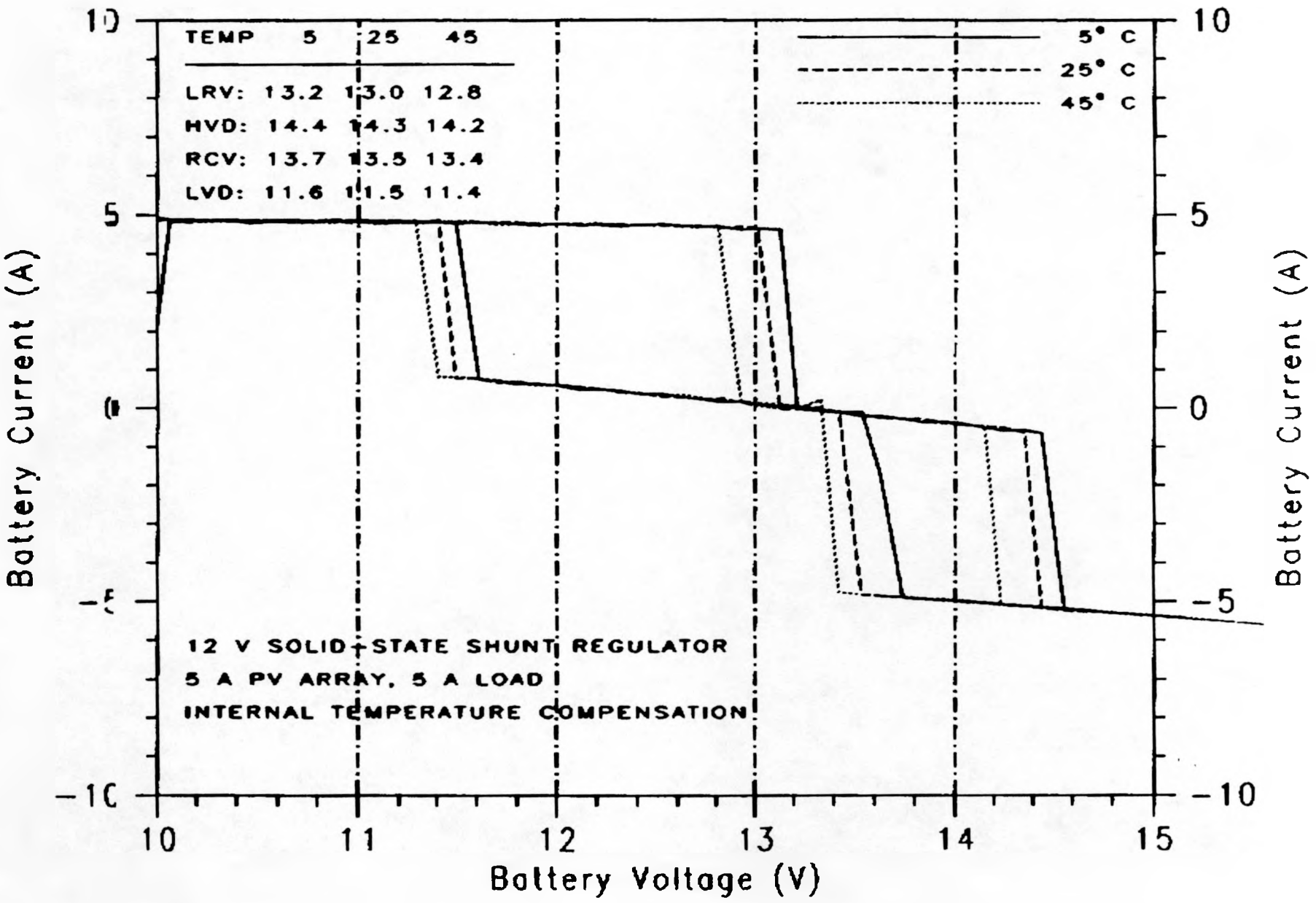
TEMP 5 25 45
LRV: 13.2 13.0 12.8
HVD: 14.4 14.3 14.2
RCV: 13.7 13.5 13.4
LVD: 11.6 11.5 11.4
5° C
25° C
45° C
12 V SOLID-STATE SHUNT REGULATOR
5 A PV ARRAY, 5 A LOAD
INTERNAL TEMPERATURE COMPENSATION
Battery Current (A)
Battery Current (A)
Battery Voltage (V)
10
5
0
-5
-10
10
11
12
13
14
15

Fig 6

Fig 7

FV courses

Fig 8

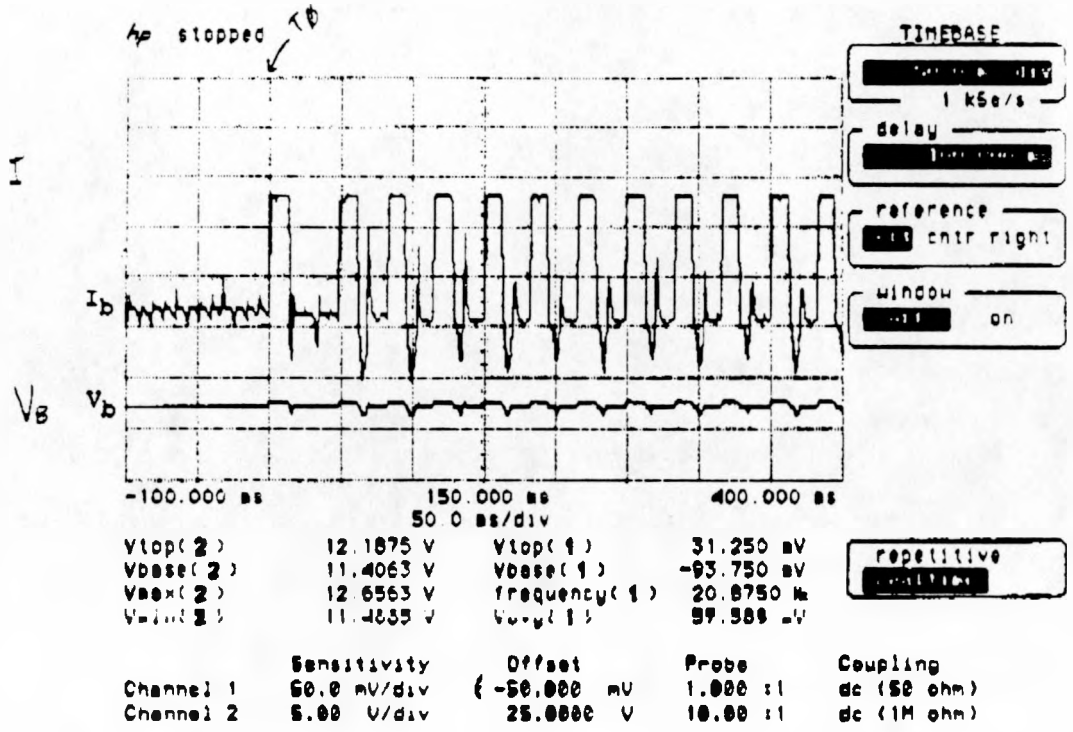

DIE HARD BATTERY, LOW SOC
THIS IS WHAT HAPPENS WHEN
YOU HIT THE LVD SET POINT.

TRIPPLITE PV250
INVERTER WITH 140W LAMP LOAD

EB SA-2

ZOC

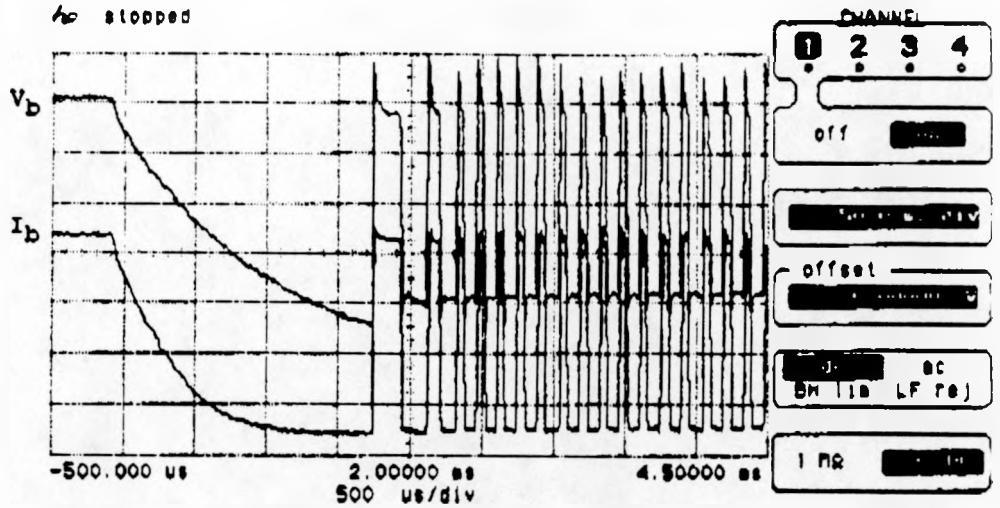

Vtop(1)	18.750 mV	Vbase(1)	-173.438mV
Vtop(2)	not found	Vbase(2)	not found
Vtop(3)	13.2969 V	Vbase(3)	11.3438 V
Vtop(4)	not found	Vbase(4)	not found

	Sensitivity	Offset	Probe	Coupling
Channel 1	50.0 mV/div	0.00000 V	1.000 :1	dc (50 ohm)
Channel 3	500 mV/div	11.7500 V	10.00 :1	dc (1M ohm)

Trigger mode : Edge
On Negative Edge Of Chan1
Trigger Level
Chan1 = -12.500 mV (noise reject OFF)
Holdoff = 40.000 ns

ARRAY 2A

DC MOTOR "ON"

IB